CrystEngComm

Accepted Manuscript

ROYAL SOCIETY OF CHEMISTRY

www.rsc.org/crystengcomm

Cite this: DOI: 10.1039/c0xx00000x

www.rsc.org/xxxxxx

ARTICLE TYPE

Fluorescence visualization of molecular assembly processes during solvent evaporation *via* aggregation-induced emission in a cyanostilbene derivative

Fuyuki Ito*[a] and Jun-ichi Fujimori[a]

Received (in XXX, XXX) Xth XXXXXXXXX 20XX, Accepted Xth XXXXXXXXX 20XX
DOI: 10.1039/b000000x

Initial stage of organic crystal formation during solvent evaporation was observed by using aggregation-induced enhanced emission, indicating fluorescence from J-aggregates was established prior to the increase in total intensity at assembly process, which suggested that the kinetics of the transformation of J-aggregates into embryonic nuclei, and subsequently to crystal can be visualized by the fluorescence.

Organic molecular materials have wide applications in electroluminescence, solar cells, and pharmaceutical products.[1, 2] Intermolecular interactions are significant factors for the development of higher functionality in these applications. To optimize the interactions, it is necessary to understand molecular packing or polymorphism during crystal growth, including nuclei formation.[3-5] To clarify crystal growth, there has been widely studied by X-ray crystallography, infrared spectroscopy, nuclear magnetic resonance, and transmission electron microscopy[6, 4].

Many organic molecules exhibit characteristic spectral changes that depend on their electronic states, how they assemble, their size, and their ambient environment.[7-9] In principle, fluorescence spectroscopy can be used to probe the progress of molecular assembly on the scale of just a few molecules or that of a bulk process. Previously, we proposed that concentration-dependent changes in fluorescence spectra for pyrene[10] and perylene[11] derivatives are observed because of matrix isolation and/or freezing of crystal nuclei growth by the polymer chains, *i.e.*, "polymer matrix isolation." In addition, we have recently reported spectroscopic changes in perylene fluorescence during solvent evaporation that provide information about molecular assembly and the nucleation and growth of crystals.[12] The quantum yield of monomer fluorescence, however, was higher than that of aggregates, which interfered with selective detection during the initial stages of molecular assembly.

Over the past decade, there have been many reports on aggregation-induced (or enhanced) emission (AIE or AIEE) in organic molecules,[13] even though the fluorescence quantum yield is low in solution, as reported by Tang *et al.*[14] AIEE enables selective detection of the assembly dynamics for aggregates and crystals. Here, for the first time, we apply AIEE to the dynamics of crystal formation. Specifically, we use a cyanostilbene derivative [1-cyano-*trans*-1,2-bis-(4'-methylbiphenyl)-ethylene (CN-MBE; Chart 1)] for AIEE, as reported by Park *et al.*[15] Using a fluorescence microscope, we characterized the spectral and intensity changes of CN-MBE emission in solutions during solvent evaporation.

CN-MBE and its nanoparticles were synthesized and prepared according to previous report, respectively.[15, 16] The solvents were 1,2-dichloroethane (DCE), dichloromethane (DCM) chlorobenzene (CB). Poly(methyl methacrylate) (PMMA), with a number-averaged molecular weight of 350,000, was purchased from Aldrich and used as received. CN-MBE-doped PMMA thin films with a PMMA concentration fixed at 2 wt% were prepared by drop-casting DCE solutions onto glass cover slips. Fluorescence spectra were recorded with a Shimadzu RF-5300PC fluorescence spectrophotometer. Droplet with 10 μL fluorescence color and intensity, as well as the morphology of the crystals, were captured with an inverted fluorescence microscope (Olympus IX71), equipped with a UPlanFl 4×/0.13 PhL (Olympus) objective lens, a CCD camera (Sigma Koki SK-TC202USB-AT), and a USB 4000 (Ocean Optics) spectrometer, which was not corrected for the wavelength dependence of the detectors. All experiments were performed at room temperature.

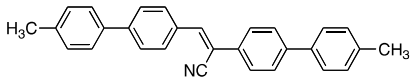

Chart 1 Molecular structure of CN-MBE.

Absorption and fluorescence spectra of CN-MBE in solutions and in nanoparticles were reported previously.[15] To suppress molecular rotation and aggregation for the observation monomer fluorescence, spectra of cast films of CN-MBE in PMMA were measured as a function of CN-MBE concentration (a polymer matrix in dilute conditions). Fig. 1 plots normalized fluorescence spectra from 330-nm excitation of these films cast from DCE solutions. At concentrations <0.1 mol%, peak emission was observed at 440 nm, with a shoulder at 420–430 nm. At increased concentrations, the fluorescence peak shifts to 470 nm and narrows. Aggregate species were observed with the fluorescence microscope at concentrations >1.0 mol% (Fig. ESI 1). Thus the spectral shift and narrowing of the fluorescence originated from CN-MBE J-aggregates.[15] To identify the emissive species at lower concentrations, excitation spectra of the CN-MBE/PMMA films were acquired (Fig. ESI 2), indicating the broad excitation spectra at 355 nm for concentrations <0.1 mol% is most likely a

combination of the planar and twisted conformers that coexist in the films as a monomer.

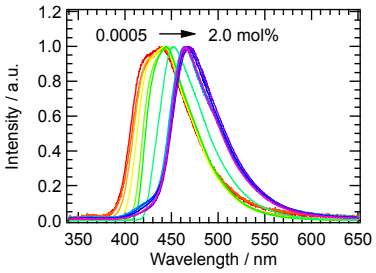

Fig. 1 Fluorescence spectra of CN-MBE in PMMA films as a function of concentration (excitation at 330 nm).

To confirm AIEE in the increased fluorescence intensity during crystal formation, we acquired fluorescence microscope images during solvent evaporation from 5.0×10^{-3} mol·dm^{-3} CN-MBE in a DCE droplet (Fig. 2). During the initial 75 s, no emission is observed from the droplet. A violet-blue feature first appeared after 90 s. More features appeared over time, aggregated around the initial feature and with increased fluorescence intensity, until the completion of evaporation at 100 s. These images indicated that CN-MBE emission in the solution phase was very weak. The polarization microscopy images were obtained with crossed Nicol polarizers indicates the crystal formation. These observations suggest that AIEE allows us to follow crystal formation by changes in fluorescence intensity. We can thus characterize the dynamics of organic crystal formation by fluorescence intensity changes.

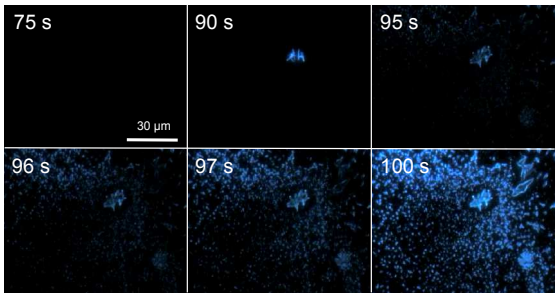

Fig. 2 Fluorescence microscope images as a function of time for 5.0×10^{-3} mol·dm^{-3} CN-MBE in a DCE droplet during solvent evaporation.

To investigate the molecular dynamics of crystal formation, fluorescence spectra were acquired during solvent evaporation for droplets of 5.0×10^{-3} mol·dm^{-3} CN-MBE in DCE (Fig. 3a). As above, the fluorescence intensity was weak just after the drop was formed. With elapsed time, the fluorescence intensity gradually increased by a factor of 100; normalized spectra are shown in Fig. 3b. After 97 s, the peak emission was at 480 nm, with a shoulder at 440 nm. Other peaks that originate from the monomer structure are observed at 443, 474, and 505 nm. The spectra become narrower with time, especially over 410–450 nm, as the solvent completely evaporates, which confirmed by microbalance. After 112 s, the spectra are identical to those in Fig. 1, suggesting that solvent evaporation results in the formation of molecular assemblies owing to increasing concentrations of CN-MBE.

The fluorescence spectra were analyzed as a function of concentration, as shown in Fig. 3c. We assumed that the spectra are from two species: a planar conformational monomer and J-aggregates. The spectrum of J-aggregates was from CN-MBE crystals. The spectrum of the planar conformational monomer was calculated from the difference between observed spectra at different time intervals. The observed spectra at each time were reproduced by non-linear least-square fitting of the summation of emission from the planer monomer and J-aggregates.

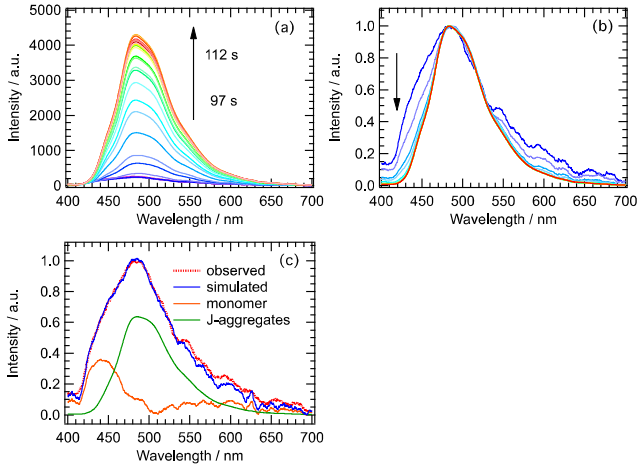

Fig. 3 Fluorescence spectral changes (a) and normalized spectra (b) of 5.0×10^{-3} mol·dm^{-3} CN-MBE in a DCE droplet during solvent evaporation as a function of time. (c) The observed spectra after 97 s and simulated spectra from summation of the relative abundance of the planar conformational monomer and the J-aggregates by least-square fitting.

Fig. 4 plots the time evolution of the total fluorescence intensity of CN-MBE and the relative abundance of J-aggregates in a DCE droplet during solvent evaporation. The total fluorescence intensity significantly and monotonically increased after 98 s, and became constant after 110 s. The relative abundance of the J-aggregates increased after 97 s and became constant (0.97) after 102 s. Therefore, the rate of J-aggregate formation is faster than the increase in total fluorescence intensity, indicating a time lag for the increase in fluorescence intensity occurs for J-aggregates. The time at which a constant fraction of J-aggregates is reached (102 s) appears to coincide with the half maximum of the total fluorescence intensity (dashed vertical line as shown in Fig. 4). As mentioned above, the total fluorescence intensity is probably attributable to the amount of CN-MBE crystals, which implies that fluorescence spectral and intensity changes reflect crystal nuclei formation and crystal growth. This phenomenon was observed not only the solvent evaporation process, but also for the water fraction dependence of the nanoparticle formation for CN-MBE (Fig. ESI 3), which supports our findings.

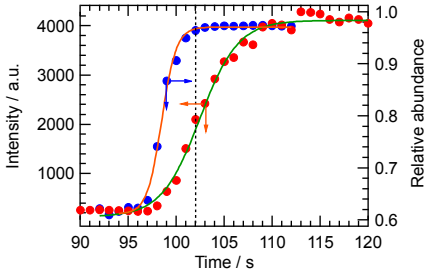

Fig. 4 Change of fluorescence intensity (red circles) and relative abundance of J-aggregate (blue circles) of CN-MBE as a function of time. The solid line is a curve fit based on the sigmoidal function (see main text).

On the basis of classical nucleation theory, the time evolution of CN-MBE fluorescence spectra during solvent evaporation can be used to model droplet growth.[4, 17] Initially, the concentration in solution was relatively low, thus an equilibrium state was established between the monomer and J-aggregates. The J-aggregates begin from the smallest cluster of two monomers formed *via* intermolecular interactions. This small cluster is unstable because of unfavorable surface free energy and dissociates before crystal formation. As the concentration increases by solvent evaporation, there are aggregate (concentration fluctuations) in supersaturated solutions. As apparent in Fig. 4, the abundance of J-aggregates during solvent evaporation indicates the formation of subcritical clusters. In general, the nucleus formation rate J is given by the Arrhenius reaction rate equation: $J=A\exp(-\Delta G/k_BT)$, where k_B is Boltzmann's constant, A is the pre-exponential factor, and ΔG is the Gibbs energy of cluster formation. Because of the energy barrier, critical nuclei formation is a competition between growth and dissolution. Therefore, the time lag between the J-aggregate abundance and the total fluorescence intensity indicates that the growth from J-aggregates to crystal nuclei is the rate-determining step of nucleation.

Amyloid fibril formation has been probed with thioflavin T (ThT) fluorescent dye[18], which is essentially nonfluorescent in solution.[19] An interaction with, or binding to, the amyloid fibril results in a fluorescence enhancement; thus ThT is a powerful tool for studying the kinetics of fibril formation, which is analogous to the organic crystal formation processes. We can use the fibrillation kinetics to model the initial stage of CN-MBE crystal formation. An sigmoidal function can be used to obtain an estimate of the time required for aggregation to level off:[20]

$$I = I_{base} + \frac{I_{max}}{1+\exp[-k(t_{half}-t)]} \quad (1)$$

where I is fluorescence intensity, I_{base} and I_{max} are, respectively, the fluorescence intensity before and after the change, k is the apparent rate constant for the growth, and t_{half} is the time to half of maximal fluorescence. The time evolution of the fluorescence intensity and the relative abundance of J-aggregates were well reproduced by Eq. 1, which parameters as depicted in Table 1. The larger values of k and t_{half} for growth of the J-aggregates relative to those for the fluorescence intensity strongly support the notion that J-aggregates act as precursors for crystal nuclei. The solvent dependence for the time evolution depends on the kinetic values associated with the boiling point and polarity of solvents, although it did not depend on the sigmoidal behaviour (Fig. ESI 4). It is suggested the molecular assembly kinetics are most probably governed increasing of local concentration in the droplets. The initial stages of crystal nuclei and crystal formation processes are schematically depicted in Fig. 5.

Table 1 Rate constant and time to half of maximum fluorescence intensity of crystal formation process for CN-MBE during the solvent evaporation from fitting of fluorescence intensity change.

Solvent (b.p.)	J-aggregates		Total intensity	
	k_J / s^{-1}	t_{half} / s	k_{Cryst} / s^{-1}	t_{half} / s
DCE (83.5 °C)	0.76	98.5	2.03	102
DCM (40.0 °C)	0.39	54.1	1.74	58.9
CB (132 °C)	1.72	678	3.57	683

The k_J and k_{Cryst} correspond to J-aggregates and crystal growth rate constants. The b.p. indicates boiling point of the solvents.

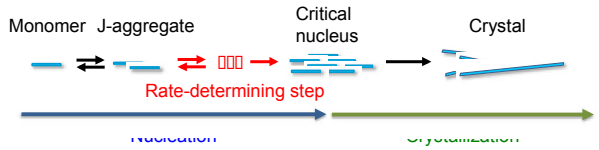

Fig. 5 Schematic of CN-MBE crystal formation based on changes in fluorescence spectra.

In conclusion, we have applied AIEE to the visualization of crystal formation processes. We found that J-aggregates act as precursors for crystal nuclei and the growth from J-aggregates to crystal nuclei is the rate-determining step in the nucleation process. The methodologies discussed here can be used to understand growth kinetics from monomer to crystal *via* crystal nuclei, which are required for organic crystal growth in real time.

The authors thank Dr. Kennosuke Itoh (Shinshu University) for the NMR measurements. This work was partly supported by the Nanotechnology Platform Program and a Grant-in-Aid for Young Scientists (B) (No. 21750021) from the MEXT of the Japanese Government, by the Iketani Science and Technology Foundation, and by the JGC-S Scholarship Foundation.

Notes and references

[a] Department of Chemistry, Faculty of Education, Shinshu University, 6-ro, Nishinagano, Nagano 380-8544, Japan. Fax: +81-26-238-4114; Tel: +81-26-238-4114; E-mail: fito@shinshu-u.ac.jp

† Electronic Supplementary Information (ESI) available: [Fluorescence microscopy, excitation spectra, the nanoparticles of CN-MBE]. See DOI: 10.1039/b000000x/

1 M. Schwoerer and H. C. Wolf, *Organic Molecular Solids*, Wiley-VCH, Weinheim, Germany, 2007.

2 J. D. Wright, *Molecular Crystals*, Cambridge University Press, Great Britain, 1995.

3 J. Bernstein, *Polymorphism in Molecular Crystals* Oxford University Press, New York, 2008.

4 R. J. Davey, S. L. M. Schroeder and J. H. ter Horst, *Angew. Chem.-Int. Edit.*, 2013, **52**, 2166.

5 D. Erdemir, A. Y. Lee and A. S. Myerson, *Acc. Chem. Res.*, 2009, **42**, 621.

6 K. Harano, T. Homma, Y. Niimi, M. Koshino, K. Suenaga, L. Leibler and E. Nakamura, *Nature Materials*, 2012, **11**, 877.

7 H. Kasai, H. Kamatani, Y. Yoshikawa, S. Okada, H. Oikawa, A. Watanabe, O. Itoh and H. Nakanishi, *Chem. Lett.*, 1997, 1181.

8 T. Tachikawa, H. R. Chung, A. Masuhara, H. Kasai, H. Oikawa, H. Nakanishi, M. Fujitsuka and T. Majima, *J. Am. Chem. Soc.*, 2006, **128**, 15944.

9 T. Asahi, T. Sugiyama and H. Masuhara, *Acc. Chem. Res.*, 2008, **41**,

1790.
10 F. Ito, T. Kakiuchi, T. Sakano and T. Nagamura, *Phys. Chem. Chem. Phys.*, 2010, **12**, 10923.
11 F. Ito, Y. Ugachi and T. Sasaki, *Chem. Lett.*, 2012, **41**, 282.
12 F. Ito, Y. Kogasaka and K. Yamamoto, *J. Phys. Chem. B*, 2013, **117**, 3675.
13 B. Z. Tang and A. Qin, *Aggregation-Induced Emission: Fundamentals*, John Wiley & Sons, Inc., United Kingdom, 2013.
14 Y. N. Hong, J. W. Y. Lam and B. Z. Tang, *Chem. Soc. Rev.*, 2011, **40**, 5361.
15 B. K. An, S. K. Kwon, S. D. Jung and S. Y. Park, *J. Am. Chem. Soc.*, 2002, **124**, 14410.
16 B. K. An, D. S. Lee, J. S. Lee, Y. S. Park, H. S. Song and S. Y. Park, *J. Am. Chem. Soc.*, 2004, **126**, 10232.
17 T. Okutsu, *J. Photochem. Photobiol. C*, 2007, **8**, 143.
18 J. N. Buxbaum and R. P. Linke, *J. Mol. Biol.*, 2012, **421**, 142.
19 V. I. Stsiapura, A. A. Maskevich, V. A. Kuzmitsky, V. N. Uversky, I. M. Kuznetsova and K. K. Turoverov, *J. Phys. Chem. B*, 2008, **112**, 15893.
20 L. Nielsen, R. Khurana, A. Coats, S. Frokjaer, J. Brange, S. Vyas, V. N. Uversky and A. L. Fink, *Biochemistry*, 2001, **40**, 6036.

Table of Contents